Modification of metal/semiconductor junctions by self-assembled monolayer organic films

Fahrettin Yakuphanoglu [a,*], Salih Okur [b], Hüseyin Özgener [c]

[a] Physics Department, Faculty of Arts and Sciences, Firat University, 23169 Elazig, Turkey
[b] Department of Physics, Faculty of Science, Izmir Institute of Technology, Gulbahce Campus, Urla, Izmir 35430, Turkey
[c] Department of Chemistry, Faculty of Science, Izmir Institute of Technology, Gulbahce Campus, Urla, Izmir 35430, Turkey

ARTICLE INFO

ABSTRACT

Two new metal/molecule/semiconductor contacts, Au/n-Si/TDA/Au and Au/p-Si/ODM/Au, were fabricated to understand effect of organic compounds, tridecylamine and octadecylmercaptan self-assembled monolayer (SAM) films, on electrical charge transport properties of the metal/semiconductor junctions. The morphology of the organic monolayers deposited on Si substrates was investigated by atomic force microscopy. The molecular coverage of ODM deposited on p-Si is poorer than that of TDA on n-Si substrate. The ideality factors of the p-Si/ODM and n-Si/TDA diodes were found to be 1.66 and 1.48, respectively. The electrical results show that the tridecylamine monolayer passivated junction has a lower ideality factor. The ideality factor indicates clear dependence on two different type functional groups R-SH (Thiol) and R-NH$_2$ (Amin) groups and it increases with different functional groups of organic molecule. The barrier height φ_b value of the n-Si/TDA diode is smaller than that of p-Si/ODM diode, as a result of chain length of the SAM organic molecules. The interface state density D_{it} values of the diodes were determined using conductance technique. The n-Si/TDA diode has the smaller interface state density according to p-Si/ODM diode.

We have evaluated that the organic molecules control the electronic parameters of metal/semiconductor diodes and thus, organic modification helps to get one step closer towards to new organic assisted silicon based microelectronic devices.

© 2009 Elsevier B.V. All rights reserved.

1. Introduction

The charge transport properties of metal–semiconductor interfaces can be controlled by use of organic molecules because of the molecules functional variety and flexibility [1]. The controlling metal–semiconductor contacts can be achieved by inserting monolayers of systematically varying molecules at their interfaces [1–4]. Organic monolayers have been used for several potential electronic applications such as molecular switches [5,6] and memory cells [7,8] molecular rectifying diodes [9–15]. When organic SAM molecules are grafted on semiconductor surface, this process modifies the electrical potential at the interface. Hence, the interface and electrical properties can be changed with respect to degree of control over the metal–semiconductor device's charge transport before contact [16–18].

In present work, we conclude that the electrical properties of silicon/metal junctions can be controlled using SAM organic molecules. We report present study to help to understand the current–voltage rectification behavior of Si/SAM/metal junctions and control of metal/semiconductor interfaces for the development of new metal–semiconductor devices.

2. Experimental details

The self-assembled monolayer (SAM) organics, tridecylamine (TDA): $C_{13}H_{29}N \cdot CH_3(CH_2)_{12}NH_2$ with 98% purity, and octadecylmercaptan (ODM): $C_{18}H_{38}S \cdot (CH_3(CH_2)_{17}SH)$ with 98% purity were purchased from Aldrich. The Au/n-Si/TDA/Au and Au/p-Si/ODM/Au diodes were fabricated using n-type and p-type single side polished single crystal silicon wafer with $\langle 1\,0\,0 \rangle$ surface orientations, 0.53 μm thick, 100 mm diameter and 2.0 Ω cm resistivity, purchased from Si-Mat Silicon Wafers Company, CZ. The Si wafers were cleaned in boiling trichloroethylene, acetone and ethanol for by 10 min, consecutively. The natural SiO$_2$ layer was removed by immersing the commercial Si wagers in CCl4, H_2SO_4, H_2O_2 and 20%HF solutions, then 6HNO$_3$:1HF:35H$_2$O and 20%HF solutions. The Si wafers were thoroughly rinsed in de-ionized water of 18 MΩ for 30 s and were dried in N$_2$ atmosphere. Self-assembled monolayer technique was applied to form both organic monolayer

* Corresponding author. Tel.: +90 424 2370000/6591; fax: +90 424 2330062.
E-mail address: fyhan@hotmail.com (F. Yakuphanoglu).

films and 1 mM SAM (TDA and ODM) solutions were prepared in ethanol. An n-type Si substrate was dipped into 1 mM TDA-ethanol solution, while a p-type Si substrate was dipped into 1 mM ODM-ethanol solution and kept them 72 h inside to form SAM monolayer on the substrates. The excess molecules were firstly removed by rinsing in clean ethanol and then cleaning in the stream of pressurized N_2 gas several times. The SAM coated films were dried and stored in Ar filled desiccators.

A high purity Au metal (99.9%) was thermally evaporated to form the top contact with a thickness of 200 nm on the TDA and ODM monolayer films deposited onto Si wafers in the pressure of 5×10^{-6} Torr. The back side of the Si substrate was polished with a high speed rotating sand paper to remove the native oxide and Au contacts were formed. The TDA on n-type Si and ODM on p-type Si were visualized with a Solver P47H atomic force microscope (NT-MTD, Moscow, Russia) operating in the tapping mode at room temperature. The average thicknesses of the SAM films were measured using AFM scratch and measure method. A scanner was used for surface morphology and phase images of the SAM films on the substrates. The images were processed by linear flattening method in order to remove the background slope. The Nova 914 software package was used for controlling the SPM system and analyzing the AFM images.

The current–voltage (I–V) characteristics of the Au/n-Si/TDA/Au and Au/p-Si/ODM/Au diodes were performed with 2400 KEITHLEY sourcemeter and GPIB data transfer card for current–voltage measurements. The capacitance–voltage measurements were measured using a 3532 HIOKI HITESTER LCR. The schematic cross-sections of the diodes are shown in Fig. 1.

3. Results and discussion

3.1. AFM results of the TDA and ODM thin films deposited on Si substrates

The AFM morphology of the TDA SAM monolayer deposited on n-Si substrate is given in Fig. 2a. The TDA molecules covered homogenously the surface with a small defect distribution where the RMS surface roughness is measured as 0.42 nm. The thickness of the monolayer was measured as 1.2 nm from the height profile of a defect or a pinhole on the film surface, as shown in Fig. 2b. A scratch lithography test in contact mode AFM was done on the SAM coated n-Si surface. Not to scratch the substrate, a safe tip pressure (3 nA cantilever deflection photocurrent signal) on a bare n-Si wafer was obtained firstly before the scratch process on the

SAM film. The scratch trace is barely visible from the AFM picture taken just after the process as given in Fig. 2c. This shows that the TDA molecules are strongly bound to the n-Si semiconducting surface, since the applied tip force could not remove the TDA molecules. The TDA molecules bound covalently over the –NH₂ head groups to the Si surface or to a thin native SiO_2 layer on the Si substrate created before the SAM film formation. The lack of debris of TDA molecules after the contact mode AFM tip scratch is another confirmation of this idea, as seen in AFM phase image of the same scratched region given in Fig. 2d. The applied tip force can just cause bending of TDA molecules in the path of contact AFM tip during scratch process.

The AFM morphology of the ODM SAM monolayer deposited on p-type Si substrate is given in Fig. 3a. The coverage of ODM molecules is not similar to the TDA film. There are molecular agglomerations with large defect distributions, where the RMS surface roughness is measured as 1.87 nm. The thickness of the agglomerated ODM layer was found to be about 5 nm from the height profile of a defect on the film surface as shown in Fig. 3b. Similar scratch lithography test in contact mode, AFM was done on the ODM SAM coated p-Si surface. A square of 1 μm area is scanned in contact mode with a safe tip force (the same cantilever deflection photocurrent signal) obtained on a bare p-Si wafer before the contact mode scan. The AFM picture taken just after the process given in Fig. 3c shows a clearly visible scan trace. That means the ODM molecules are not or loosely bound to the p-Si semiconducting surface, since there is no ODM SAM layer left in the scanned region. All the molecules are collected and dropped outside the region by the AFM tip during the scan in contact mode. The –SH head groups of ODM molecule are not bound to the Si or Si/SiO_2 surface. The collected debris of ODM molecules outside the scan region confirms this idea, as seen in AFM phase image of the same scan region given in Fig. 3d.

3.2. The current–voltage characteristics of p-Si/ODM and n-Si/TDA diodes

The energy band diagrams of prepared organic-on-inorganic semiconductor (OI) diodes are shown in Fig. 4a and b. We have evaluated that the fabricated OI structures behave like a metal/semiconductor Schottky contact. Fig. 5 shows the current–voltage characteristics of the p-Si/ODM and n-Si/TDA diodes passivated by tridecylamine (TDA) ($C_nH_{2n+3}N$, $n = 13$) and octadecylmercaptan (ODM) ($C_nH_{2n+2}S$, $n = 18$) organic molecules. The diodes show a good rectifying behavior with TDA and ODM molecules. I–V
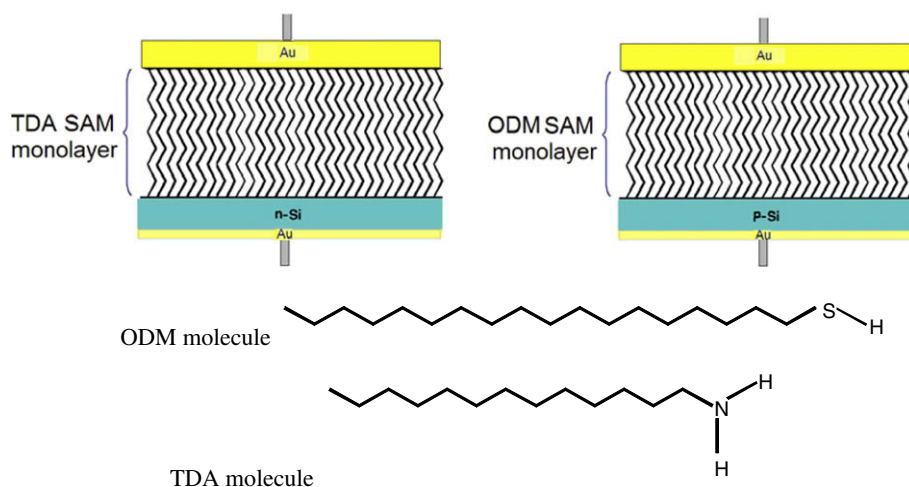

Fig. 1. Modification of the organic molecules to silicon surface.
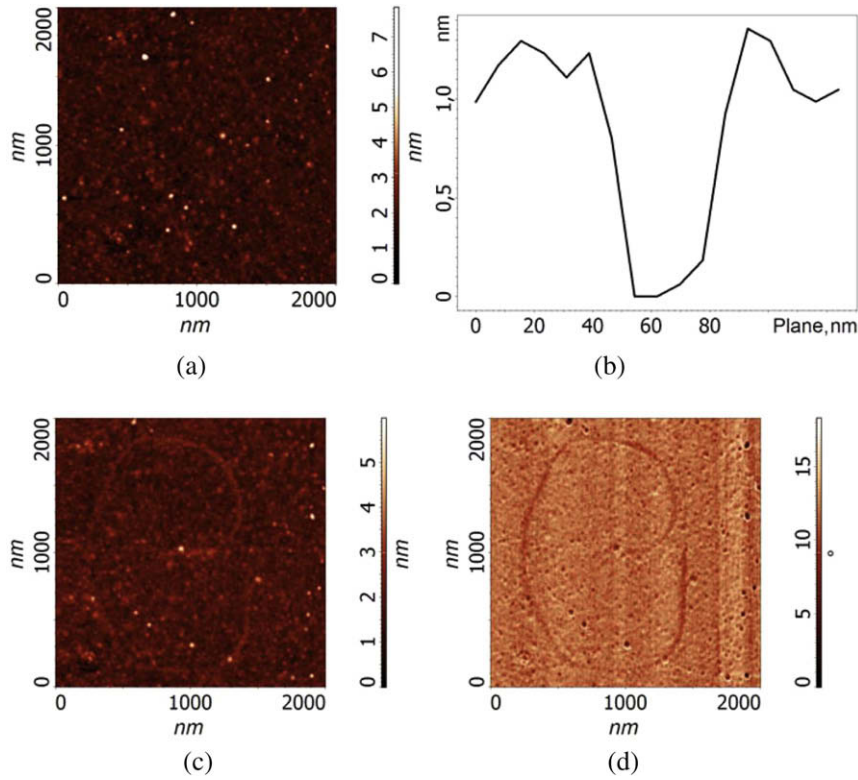
Fig. 2. (a) The AFM morphology of the TDA SAM monolayer surface on n-Si substrate, (b) the height profile of a defect or a pinhole on the film surface taken for the thickness measurements of the monolayer film, (c) AFM picture of a scratch lithography test in contact mode AFM, and (d) the AFM phase image of the same scratched surface.
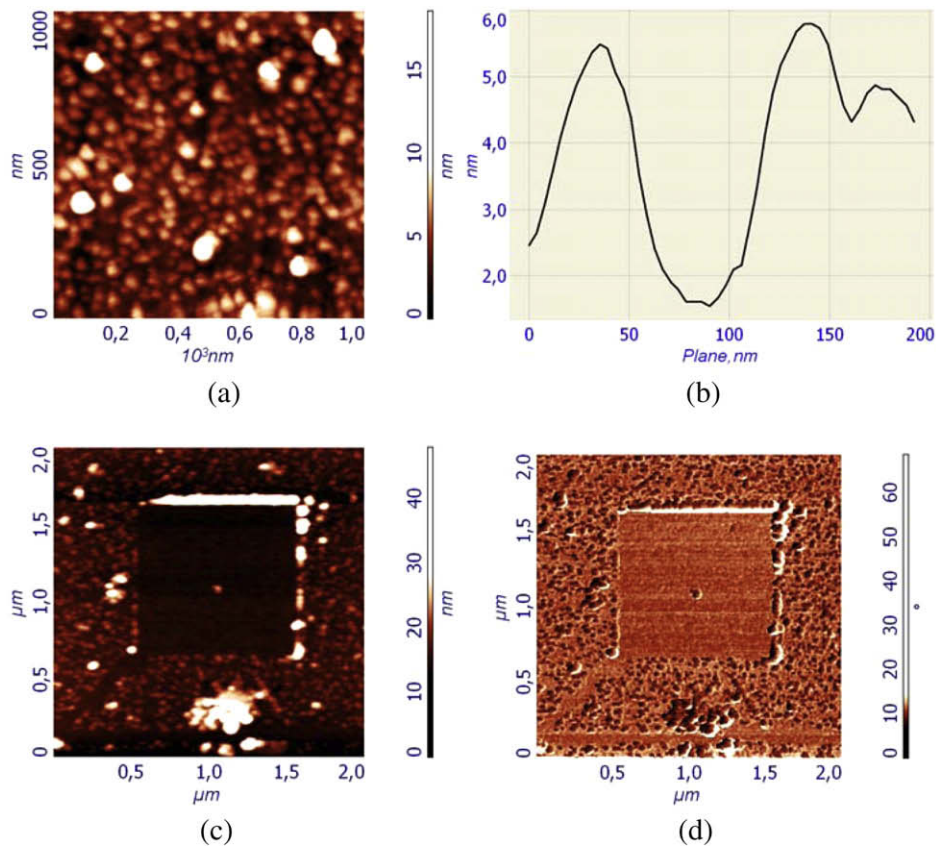

Fig. 3. (a) The AFM morphology of the ODM SAM monolayer surface on p-type Si substrate, (b) the height profile of a defect on the agglomerated ODM film surface taken for the thickness measurements of the monolayer film, (c) AFM picture of a scan test in contact mode, and (d) the AFM phase image of the same scan region.
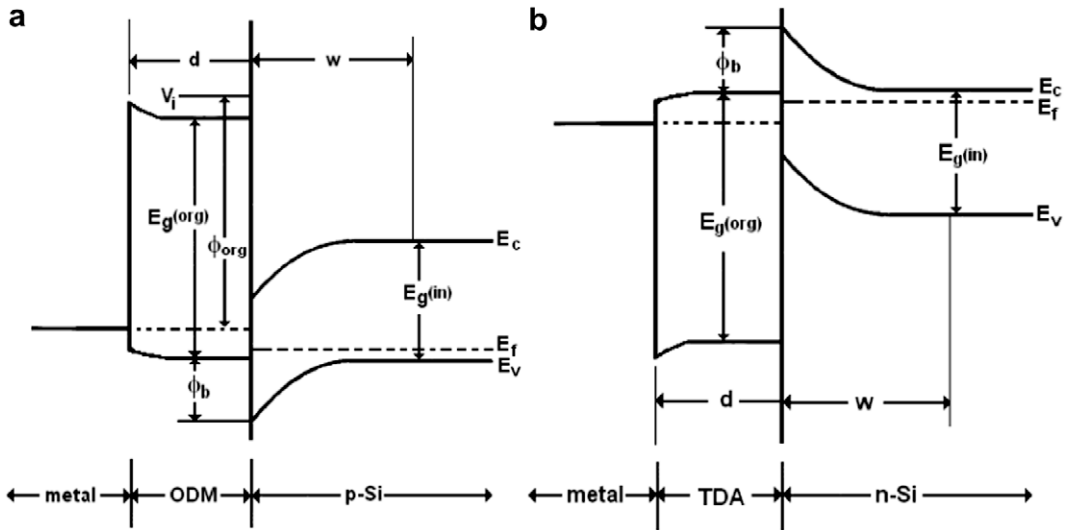
a

b

Fig. 4. Energy-band diagrams of the diodes (a) p-Si/ODM (b) n-Si/TDA. E_f is the Fermi level, d is the thickness of organic layer interfacial layer, φ_b is the barrier height, φ_{org} is the work function of the organic material, V_i is the potential drops across the interfacial layer, E_g(org) is the band gap of the organic material, E_g(in) is the band gap of inorganic semiconductor, w is the width of the depletion region.
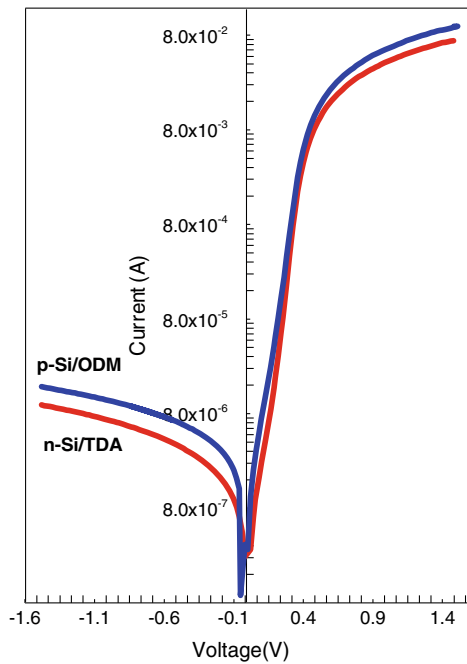

Fig. 5. Current–voltage characteristics of the p-Si/ODM and n-Si/TDA diodes.

characteristics of an organic molecule inserted between metal and semiconductor junction can be analyzed by the following relation [19]

$$I = AA^*T^2 \exp\left(-\beta d\right) \exp\left(-\frac{q\phi_b}{kT}\right) \exp\left(\frac{qV}{nkT}\right)\left[1 - \exp\left(-\frac{qV}{kT}\right)\right] \tag{1}$$

where A is the contact area, A^* is the Richardson constant (112 A/cm^2 K^2 for n-Si and 32 A/cm^2 K^2 for p-Si) [20], T is the temperature, φ_b is the barrier height and β is the tunneling constant. When an organic layer with d thickness is inserted between metal and semiconductor, the effective barrier height is defined as [19]

$$\phi_{eff} = \phi_b + \frac{kT\beta d}{q} \tag{2}$$

If Eq. (1) is rearranged, one obtains

$$I = AA^*T^2 \exp\left(-\frac{q\phi_{eff}}{kT}\right) \exp\left(\frac{qV}{nkT}\right)\left[1 - \exp\left(-\frac{qV}{kT}\right)\right] \tag{3}$$

where n is the ideality factor, which generally is higher than unity. The ideality factors of the diodes were determined from the I–V characteristics of the diodes. The obtained ideality factors are higher than unity, suggesting that the diodes indicate non-ideal behavior due to the interface layer and interface oxide layer and series resistance. Thus, for the junctions, we cannot ignore the series resistance effect and thus, Eq. (3) including series resistance can be rewritten as [21]

$$I = AA^*T^2 \exp\left(-\frac{q\phi_{eff}}{kT}\right) \exp\left(\frac{q(V - IR_s)}{nkT}\right) \quad \text{for} \quad q(V - IRs) > kT \tag{4}$$

If one rearranges Eq. (4), it gives

$$V = n\frac{kT}{q} \ln\left(\frac{I_o}{AA^*T^2}\right) + IR_s + n\phi_{eff} \tag{5}$$

If Eq. (5) is differentiated with respect to I, one obtains

$$\frac{dV}{d\ln(I)} = n\frac{kT}{q} + IR_s \tag{6}$$

and a $H(I)$ function can be defined as follows

$$H(I) = V - n\frac{kT}{q} \ln\left(\frac{I_o}{AA^*T^2}\right) = IR_s + n\phi_{eff} \tag{7}$$

where I_o is the saturation current, A is the contact area, R_s is the series resistance and φ_b is the barrier height. Fig. 6a and b shows the plots of $dV/d\ln I$ vs. I and $H(I)$ vs. I for the diodes. The electrical parameters of the diodes determined from these plots are given in Table 1. The ideality factors of the p-Si/ODM and n-Si/TDA diodes were found to be 1.66 and 1.48, respectively. This indicates that electronic performance of the n-Si/TDA diode is better than that of p-Si/ODM diode. It is seen that the ideality factor shows clear dependence on chain length. It increases with longer chain length, since TDA and ODM organic molecules on silicon changes the interfacial nature of metal/semiconductor contact. Although the obtained series resistance for the p-Si/ODM diode is lower than n-Si/TDA diode, the p-Si/ODM diode gives the higher ideality factor.
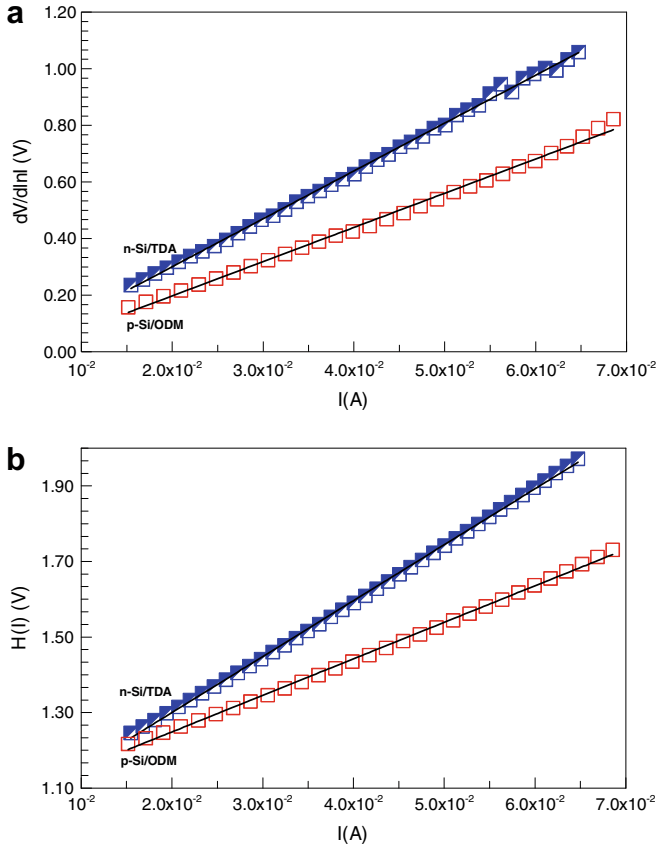
Fig. 6. Plots of $dV/d\ln(I)$ vs. I and $H(I)$ vs. I of the p-Si/ODM and n-Si/TDA diodes.

Fig. 7. Plots of C^{-2}–V of the p-Si/ODM and n-Si/TDA diodes.

The ideality factor of the n-Si/TDA/Au diode is higher than that of Au/n-Si Schottky barrier, whereas the barrier height is lower [22]. This suggests that the ideality factor and barrier height values of n-Si/TDA/Au diode are modified by coating the TDA film on silicon. The coating of SMA layer on Si wafers causes a decrease or increase in the reverse bias current of the diode and in turn, the barrier height increases or decreases. The ideality factor of Au/p-Si/ODM/Au diode is lower than that of Au/p-Si/strontium titanate(STO)/Au diode [23], whereas the barrier height is higher. We evaluate that the pure contacts of Au/p-Si and Au/n-Si show the similar Schottky behavior without organic SAM molecule.

3.3. Capacitance–voltage characteristics of the p-Si/ODM and n-Si/TDA diodes

The capacitance–voltage (C–V) characteristics of the p-Si/ODM and n-Si/TDA diodes under 100 kHz were performed to get the detailed information about the electrical characteristics of the diodes and the obtained C–V curves of the diodes were analyzed by the following relation [20]

$$\frac{1}{C^2} = \frac{2(V_{bi}+V)}{A^2 \varepsilon_o \varepsilon_s q N_{d,a}} \qquad (8)$$

where V_{bi} is the built-in potential, ε_o is the permittivity of free space, ε_s is the dielectric constant of semiconductor, $N_{d,a}$ is the carrier con-

centration and d, and a subscripts refer to donor and acceptor concentrations, respectively. In order to obtain diode parameters, the C–V curves were plotted in the form of C^{-2}–V and the plots are given in Fig. 7. As seen in Fig. 7, the plots show linear dependence over a large voltage range. The V_{bi} and $N_{d,a}$ values for the p-Si/ODM and n-Si/TDA diodes were determined from intercept and slopes of Fig. 7 and the obtained results are given in Table 1. The barrier height φ_b of the diodes can be determined by the following relation

$$q\phi_{B(C-V)} = qV_{bi}/n + kT \ln\left(\frac{N_{c,v}}{N_{d,a}}\right) \qquad (9)$$

where $N_{c,v}$ is the effective density of state in the electronic bands of silicon ($N_v = 1.82 \times 10^{19}$ cm^{-3} for Si and $N_c = 2.78 \times 10^{19}$ cm^{-3}) [20] and subscripts c and v refer to conduction and valance band, respectively. The $N_{d,a}$, V_{bi} and φ_b values of the diodes were determined from C–V characteristics and the results are presented in Table 1. The φ_b value of the n-Si/TDA diode is lower than that of p-Si/ODM diode as a result of chain length difference of the SAM organic molecules. These capacitance results indicate that the organic SAM modification does not alter the intrinsic properties of the silicon substrate.

3.4. Determination of interface state density of the n-Si/TDA and p-Si/ODM diodes

The interface states affect the device performance of metal–semiconductor junctions. Therefore, it is very important to determine the interface state density of the n-Si/TDA and p-Si/ODM diodes. For the determination of the interface state density, we use the conductance technique suggested by Nicollian and Brews. In this method, the interface state conductance for the diodes is expressed by the following relation [24]

$$\frac{G_p}{\omega} = \frac{qAD_{it}\tau}{2\omega\tau} \ln(1 + \omega^2\tau^2) \qquad (10)$$

where D_{it} is the density of the interface states, τ is the time constant of the interface states q is the charge of the electron and ω is the angular frequency. In the conductance method, G_p/ω vs. ω curves usually gives a peak and thus, interface state density is determined by means of this peak

Table 1
Electronic parameters of the p-Si/ODM and n-Si/TDA diodes.

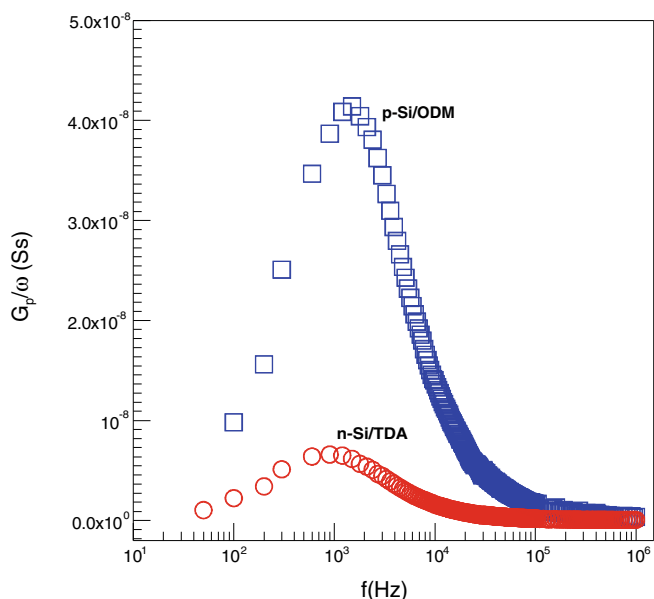| Diode	$^{dV/d\ln I}n$	$^{dV/d\ln I}R_s$ (Ω)	$^{H(I)}\varphi_b$ (eV)	V_{bi} (V)	$^{C-V}\varphi_b$ (eV)	$N_{d,a}$ (cm^{-3})	$^{H(I)}R_s$ (Ω)	D_{it} (eV cm^{-2})
n-Si/TDA	1.48	16.92	0.67	0.86	0.79	6.45×10^{15}	14.81	3.36×10^{12}
p-Si/ODM	1.66	12.09	0.63	0.88	0.73	6.52×10^{15}	9.67	4.15×10^{13}

Fig. 8. Plots of G_p/ω-f of the p-Si/ODM and n-Si/TDA diodes.

$$D_{it} = \frac{(G_p/\omega)_{max}}{0.402qA} \tag{11}$$

For determination of the interface state density of the diodes, we measured the conductance as a function of frequency and the plots of G_p/ω vs. f are shown in Fig. 8. As seen in Fig. 8, the n-Si/TDA diode has the smaller peak height compare to p-Si/ODM diode. This suggests that the interface state density of n-Si/TDA diode is smaller than that of p-Si/ODM diode. The obtained D_{it} values for the diodes are given in Table 1. It reveals that use of organic molecules changes the interfacial nature of metal/semiconductor diodes. As seen in Table 1, the effective barrier height of n-Si/TDA diode is higher than that of p-Si/ODM. This indicates that lower interface state density gives higher barrier height.

4. Conclusions

The electrical characterization of the metal/molecule/semiconductor junctions were investigated by current–voltage, impedance spectroscopy and AFM techniques. The molecular coverage of ODM and TDA molecules n-Si substrates were examined by atomic force microscopy. The AFM results show that the TDA SAM molecules covered the n-Si surface homogenously with smaller defect distribution to compare ODM on p-Si surface. The rms surface rough-

nesses of TDA and ODM SAM moleculer films are measured as 0.42 nm and 1.87, respectively. The AFM contact mode scratch test shows that TDA SAM molecules bound strongly to the n-Si substrate, while ODM SAM molecules are loosely bound to the p-Si semiconducting surface.

The ideality factor, barrier height and interface state density values of the p-Si/ODM and n-Si/TDA diodes were determined to obtain the effect of organic modification on the metal/semiconductor interfaces. The surface and electrical characterization results show that the self-assembled monolayer molecules control the electronic parameters of metal/semiconductor junctions.

References

[1] A. Vilan, A. Shanzer, D. Cahen, Nature 404 (2000) 166.
[2] J. Krüger, U. Bach, M. Gratzel, Adv. Mater. 12 (2000) 447.
[3] F. Nuesch, F. Rotzinger, L. Si-Ahmed, L. Zuppiroli, Chem. Phys. Lett. 288 (1998) 861.
[4] A. Ulman, An Introduction to Ultrathin Organic Films: From Langmuir–Blodgett to Self-assembly, Academic Press, Boston, 1991.
[5] C.P. Collier, G. Mattersteig, E.W. Wong, Y. Luo, K. Beverly, J. Sampaio, F. Raymo, J.F. Stoddart, J.R. Heath, Science 289 (2000) 1172.
[6] A.R. Pease, J.O. Jeppesen, J.F. Stoddart, Y. Luo, C.P. Collier, J.R. Heath, Acc. Chem. Res. 34 (2001) 433.
[7] J. Chen, M.A. Reed, A.M. Rawlett, J.M. Tour, Science 286 (1999) 1550.
[8] M.A. Reed, J. Chen, A.M. Rawlett, D.W. Price, J.M. Tour, Appl. Phys. Lett. 78 (2001) 3735.
[9] A. Aviram, M.A. Ratner, Chem. Phys. Lett. 29 (1974) 277.
[10] G.J. Ashwell, J.R. Sambles, A.S. Martin, W.G. Parker, M. Szablewski, J. Chem. Soc., Chem. Commun. (1990) 1374.
[11] A.S. Martin, J.R. Sambles, G. Ashwell, J. Phys. Rev. Lett. 70 (1993) 218.
[12] R.M. Metzger, B. Chen, U. Hopfner, M.V. Lakshmikantham, D. Vuillaume, T. Kawai, X. Wu, H. Tachibana, T.V. Hughes, H. Sakurai, J.W. Baldwin, C. Hosch, M.P. Cava, L. Brehmer, G.J. Ashwell, J. Am. Chem. Soc. 119 (1997) 10455.
[13] D. Vuillaume, B. Chen, R.M. Metzger, Langmuir 15 (1999) 4011.
[14] R.M. Metzger, T. Xu, I.R. Peterson, J. Phys. Chem. B 105 (2001) 7280.
[15] T. Xu, I.R. Peterson, M.V. Lakshmikantham, R.M. Metzger, Angew. Chem. Int. Ed. Engl. 40 (2001) 1749.
[16] D. Cahen, A. Kahn, E. Umbach, Mater. Today 8 (2005) 32.
[17] K.W. Hipps, Science 294 (2001) 536.
[18] J.G. Kushmerick, Mater. Today 8 (2005) 26.
[19] Y. Selzer, A. Salomon, D. Cahen, J. Phys. Chem. B 106 (2002) 10432.
[20] M. Sze, Physics of Semiconductor Devices, Wiley, New York, 1981.
[21] S.K. Cheung, N.W. Cheung, Appl. Phys. Lett. 49 (1986) 85.
[22] M. Sağlam, F.E. Cimilli, A. Türüt, Physica B 348 (2004) 397.
[23] R.K. Gupta K. Ghosh, P.K. Kahol, Curr. Appl. Phys. 9 (2009) 673.
[24] E.H. Nicollian, J.R. Brews, MOS (Metal Oxide Semiconductor) Physics and Technology, Wiley, New York, 1982.